Theoretical study of hydrogen adsorption on FePd face-centered cubic alloy surfaces

Paula V. Jasen, Estela A. Gonzalez, Norberto J. Castellani, and Alfredo Juan*
Departamento de Física, Universidad Nacional del Sur, Av. Alem 1253, Bahía Blanca (8000), Argentina
(Received 18 June 2004; revised manuscript received 27 September 2004; published 29 June 2005)

Adsorption of hydrogen on the ordered FePd face-centered cubic (fcc) alloys was investigated using a tight binding theoretical method and a five-layer slab surface model. The calculations predict that hydrogen is bonded mainly to Pd atoms, while the metal–metal bonding is almost not affected on the fcc surfaces. The changes in the electronic structure and bonding in the (100), (110), and (111) surfaces were also analyzed. The H–surface bond is achieved at the expense of the metal–metal bond. The results are compared with previous studies on FePd face-centered tetragonal (fct) surfaces and FePd bulk structures.

DOI: 10.1103/PhysRevB.71.235422 PACS number(s): 73.20.At, 71.20.Be

I. INTRODUCTION

There are many processes in the petrochemical and fine-chemical synthesis industry that are carried out over supported bimetallic catalysis.[1]

It is well known that the changes in the electronic structure of a Pd (111) surface, through alloying with an early transition metal (TM), have dramatic effects on its surface chemical reactivity.[2]

Nowadays, great attention has been paid to binary and ternary Pd alloys.[3] Hayashi *et al.* have reported experiments where Pd-coated Fe films show practically null permeability to hydrogen.[4–7] That is the reason why interfacial Fe-Pd studies have a critical technological importance. Furthermore, Fe-Pd multilayers are of particular interest because of an abnormal Pauli susceptibility of the Pd atoms. There is no visible interdiffusion of Fe into the Pd layers either. However, at higher growth temperatures an essential interdiffusion of Fe into Pd has been reported.[8]

The interactions of hydrogen with the B2TiFe surfaces and the changes in the electronic structure have been reported by Lee *et al.*[9] It is assumed that Pd coating or alloying will be beneficial for hydrogen uptake because the Pd is a catalytically active element.[10] The absorption of hydrogen on TiFe surface covered by a Pd monolayer has been studied using the full potential augmented plane wave method (FPLAPW). The results show that in all considered cases H is located below the Pd surface. Furthermore, hydrogen located between Fe atoms can cause a weakening of the interatomic bonds.[11] Pd and its alloys have been extensively studied because they absorb hydrogen reversibly.[12] It is well known that Pd adsorbs hydrogen well and forms hydrides with hydrogen in both the octahedral and tetrahedral sites, and it does not readily transport oxygen.

Recently, our group has addressed the study of Fe–Pd–H system. The H-metal interaction is favored at the interface. The Fe-Fe and Pd-Pd bonds close to H are weakened, while a H–Fe and H–Pd bond is developed. The strong bonding at the Fe–Pd interface is almost unaffected by H. Regarding H diffusion, the first Pd layer stopped any further movement of the H impurity within the cluster.[13] The impurity reduces the interfacial adhesion. When alloys bulk structures are considered, hydrogen produces a notorious detrimental effect in the Pd–Pd bonds in the Fe-Pd face-centered cubic (fcc) phase, while for the face-centered tetragonal (fct) phase, the decrease in overlap populations (OP) is only about 12% for the same bond.[14] According to our calculations, the H absorption is a favorable process in both Fe-Pd alloy structures analyzed. H is more stable when it is located at the tetrahedral interstitial site in an FePd fct phase. The Pd-H computed distances are shorter than those of stoichiometric PdH_x hydride, while the Fe-H distances in the fcc structure are similar to those of the high-pressure stoichiometric hydride (FeH). Both band structures show a lower energy region where the H contribution is located. No significant changes in the metal-based bands were observed.[15]

In this study we compute the electronic structure on the one of the two stable Fe-Pd 1:1 structure by the extended Hückel tight binding method (EHTB). We discuss the interaction of the metal surface states with hydrogen and the influence of the adatom on the electronic structure and metal–metal bonding.

II. THE SURFACES MODEL

The equiatomic Fe-Pd alloys can develop two stables structure. One of them, known as the high-temperature phase, has a fcc crystal structure with a well-known NaCl-type structure and a lattice parameter $a_0=3.90$ Å (see Fig. 1).[16] The other Fe-Pd alloy structure is a CuAu(I) type with lattice parameters $a=3.86$ Å and $c=3.73$ Å.[16,17] In metallurgical nomenclature, it is known as the $L1_0$ phase. The crystal space group is $P4/mmm$.

We have studied the H absorption on the (100), (110), and (111) surfaces for the fcc alloy structure. The thickness of the slab (five layers) is such that it approximates the electronic structure of the 3D solids in the innermost layer. In a recent calculation we have computed the electronic structure of Fe-Pd alloys.[15] The present slab calculation shows a good agreement with our extended previous calculations, and our preliminary density functional theory (DFT) calculations confirm the results. On the other hand, Dominguez *et al.* have shown that larger number of atoms do not always improve the calculations of the electronic properties of the crystalline surface.[18] The surface models are shown in Fig. 1. For the ideal (111) surface of the fcc phase there are two possible terminations. It can be either pure Fe or pure Pd (see Fig. 1).

 ©2005 The American Physical Society

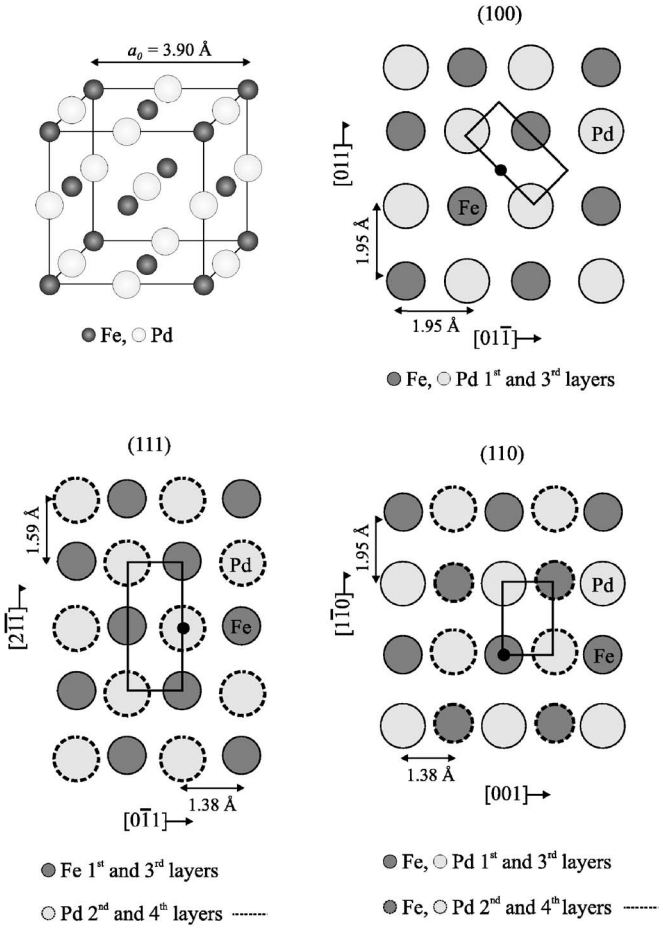

FIG. 1. FePd alloys structure for fcc phase. Schematic view of the planes (100) (only the first layer is shown; the second and fourth layers have changed the Fe and Pd locations with respect to the first layer); (111) (the third and fourth layers have the same composition as the first and second layers with a shift of 0.796 Å at [110] direction); and (110). The energy was evaluated on the region inside the box. The small circle in black indicates the H location.

On the other orientations there are always mixed FePd structures. We have mapped the H adsorption energy in each surface at 0.01 Å steps. After that, the H location was optimized.

III. RESULTS AND DISCUSSION

The most stable plane for the H adsorption is the (110) in the fcc structure (see Table I, where the energies values are relative to the minimum value for H location). Table I also shows the corresponding values for the fct structure. In both structures the $\Delta E_{\text{superficial}}$ has almost no change after H interaction. This supports the idea of a local effect of H on the metal–metal bonding. The low-H concentrations explain a slight effect on the surface energy values. In the case of alloys the phenomena of surface segregation should be mentioned. There are several models of surface segregation that mainly consider one metal as an impurity while the other metal acts as a host. Ruban *et al.* have studied the surface segregation in TM model alloys.[19] When Fe is considered an impurity in fcc Pd, it segregates towards the surface; however, when Pd is the impurity in body-centered cubic (bcc), Fe does not segregate. The surface composition of alloys has also been studied using models of nonideal solutions.[20] Segregation-energy calculations in thin films of binary fcc metal alloys and in bcc TM have been studied both theoretically and experimentally in recent years. To the best of our knowledge segregation in ordered FePd alloys has not been considered.[21,22]

TABLE I. Relative adsorption and superficial (for pure cluster and after H interaction) energies of the FePd alloys structure.

Structure	ΔE_{ads} (relative)	$\Delta E_{\text{superficial}}$ (relative)	$\Delta E_{\text{superficial with H}}$ (relative)
	FePd (fcc)		
(100)	0.71	1	1
(110)	0.99	0.35	0.351
(111) Fe term.	0.69	0.069	0.072
(111) Pd term.		0.092	0.096
	FePd (fct)		
(100)	1	0.511	0.512
(110)	0.93	0.104	0.104
(111)	0.50	0.615	0.617

It can be seen from Fig. 1 that the plane (100) is the more open surface. The adsorption geometries are different. In the plane (100), H is located in a bridge position, while for the (111) and the (110) the top adsorption is preferred. In its minimum energy H is 0.90 Å below the top metal layer at an Fe-H distance of 1.631 Å and a Pd–H of 1.647 Å. In the case of (111) surface, the H is 0.80 Å below the top metal layer which is formed by Fe atoms. H is top-bonded to a Pd atom (of the second layer) at a Pd-H distance of 1.45 Å; however, H is also close to an Fe (1.59 Å). When the (111) surface is Pd terminated, H is adsorbed at 1.54 Å from the surface, being energetically unstable at lower distances while not diffuse to the bulk. In pure fcc Pd(111) surface, Paul and Sautet have reported a Pd-H distance of 1.57 Å at the top site.[23] On the (110) surface, H is located 1.60 Å above the plane on top of an Fe atom. The closer Pd-H distance is 2.52 Å.

As mentioned before, the computed Pd-H distance on the (100) plane is 1.65 Å, which is consistent with the sum of the atomic radii. The optimum Pd–H distance obtained by LEED for the fcc Pd(111) is 1.78 Å; for a surface fcc hollow site on pure Pd(111) it ranges from 1.78 to 1.80 Å, which corresponds to a vertical height of 0.80–0.85 Å for H.[24] Experimental photoemission measurements show that the H atoms prefer the hollow site at a bonding Pd-H distance of 1.67 Å.[23] Also, our computed Pd-H distances are close to those reported by Skottke *et al.*[25] The energy difference between H on Pd(001)—at 1.6 Å above the top metal layer—and H on the alloy surface yields 0.84 eV, which means a change of 16.5%.

The computed Fe-H distance is shorter than those of H on pure bcc Fe(110).[26,27]

Let us discuss first the electronic structure of the Fe-Pd alloy free of hydrogen. In the density of states (DOS) of the

TABLE II. Electron density, overlap population, charge and distances for FePd high temperature structure (fcc).

		Electron density						
Structure		*s*	*p*	*d*	Charge	OP[a]	Distances (Å)	E_F (eV)
FePd(100)								
Fe-Fe		0.60	0.14	5.95	1.313	0.002	2.758	−7.73
Fe-Pd	Fe	0.60	0.14	5.95	1.313	0.473	1.950	
	Pd	0.91	0.97	9.26	−1.151			
Pd-Pd		0.92	0.98	9.25	−1.161	0.053	2.758	
FePd(111)								
Fe-Fe		0.72	0.05	7.64	−0.413	0.687	2.106	−8.50
Fe-Pd	Fe	0.67	0.33	5.15	1.845	0.101	2.640	
	Pd	0.75	0.76	9.44	−0.949			
Pd-Pd		0.77	0.79	9.42	−0.977	0.326	2.106	
FePd(110)								
Fe-Fe		0.67	0.24	7.44	−0.352	0.152	2.758	−7.93
Fe-Pd	Fe	0.74	0.22	8.46	−1.433	0.485	1.950	
	Pd	0.83	0.93	9.06	−0.820			
Pd-Pd		0.98	0.91	9.44	−1.332	0.058	2.758	

[a]OP: overlap population.

TABLE III. Electron density, overlap population, charge and distances for FePd high temperature structure (fcc) after H adsorption.

		Electron density							
Structure		*s*	*p*	*d*	Charge	OP[a]	%ΔOP[b]	Distances (Å)	E_F (eV)
FePd(100)-H									
Fe-H	H	1.17	0.00	0.00	−0.174	0.098	···	1.631	−7.69
	Fe	0.55	0.11	6.00	1.337				
Pd-H	Pd	0.78	0.92	9.05	−0.749	0.230	···	1.647	
Fe-Fe		0.60	0.14	5.95	1.308	0.002	···	2.758	
Fe-Pd	Pd	0.92	0.98	9.26	−1.153	0.474	···	1.950	
Pd-Pd		0.93	0.97	9.30	−1.167	0.053	···	2.758	
FePd(111)-H									
Fe-H	H	1.21	0.00	0.00	−0.216	0.217	···	1.595	−8.47
	Fe	0.51	0.14	6.34	1.016				
Pd-H	Pd	0.69	0.81	9.35	−0.849	0.338	···	1.454	
Fe-Fe		0.72	0.05	7.96	−0.434	0.687	···	2.106	
Fe-Pd	Fe	0.68	0.33	5.21	1.783	0.102	···	2.640	
	Pd	0.74	0.75	9.44	−0.938				
Pd-Pd		0.74	0.75	9.44	−0.938	0.301	−8	2.106	
FePd(110)-H									
Fe−H	H	1.49	0.00	0.00	−0.493	0.612	···	1.600	−7.91
	Fe	0.53	0.35	5.74	1.375				
Pd-H	Pd	0.83	0.84	9.20	−0.882	0.018	···	2.522	
Fe-Fe		0.67	0.24	7.45	−0.369	0.152	···	2.758	
Fe-Pd	Fe	0.75	0.22	8.47	−1.441	0.484	···	1.950	
	Pd	0.83	0.93	9.06	−0.926				
Pd-Pd		0.98	0.83	9.44	−1.333	0.058	···	2.758	

[a]OP: overlap population.

[b]%ΔOP: percentage change in the OP of a specified bond when H is absorbed. The negative signs indicate a decrease in the strength of the bond.

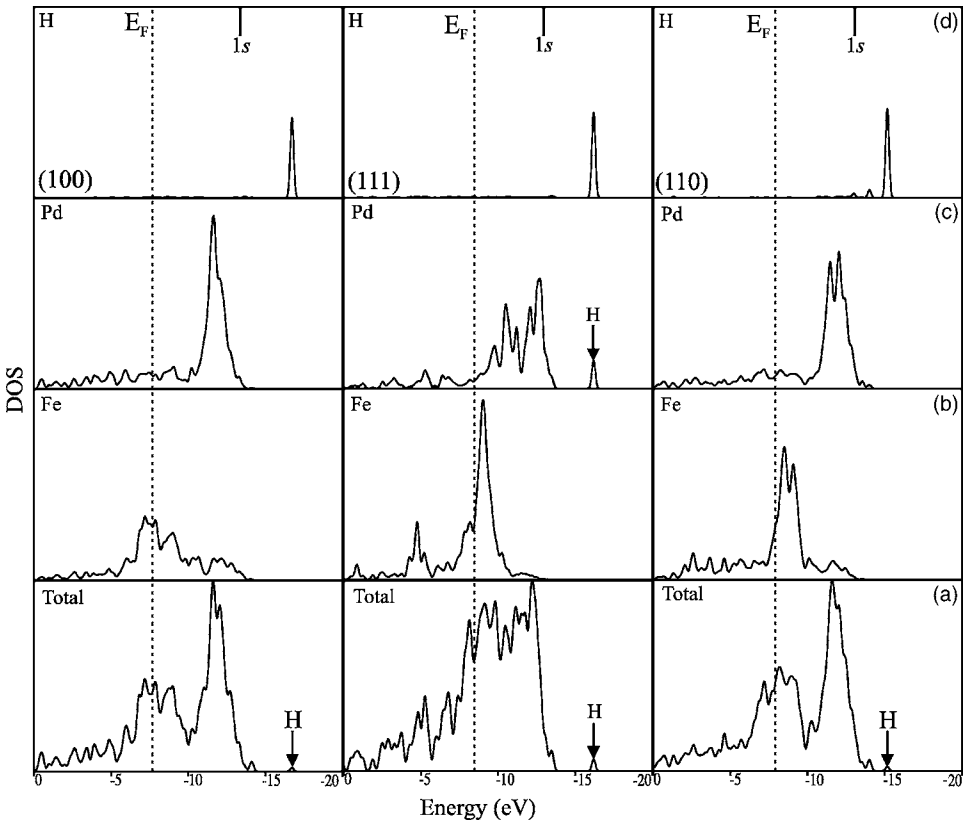

FIG. 2. Total DOS of an Fe-Pd fcc alloy with H adsorbed on the surfaces (a), projected DOS of the Fe surface atoms first neighbors to H (b), projected DOS of the Pd surface atoms first neighbors to H (c), and hydrogen projected DOS (d). The bar indicates the H 1*s* energy before adsorption.

reference bulk solids (Fe bcc and Pd fcc) the metals' *d* states form a band between −12 and −7 eV for Fe and between −13 and −10 eV for Pd.[13] The detailed compositions of states for the FePd fcc alloy are shown in Table II. In the alloy, the Fe atoms become positively charged and the Pd and H atoms negatively charged in all considered surfaces.

The orbital composition of Fe and Pd atoms shows little change after H adsorption. However, in the FePd(100)-H case the Pd 5*s* and 4*d* orbitals change by ≈−0.15 and ≈−0.25, respectively (see Tables II and III). The Fe atoms change their electronic orbital population a little in the (100) plane. However, in the (111) and (100) cases the 4*s* and 3*d* populations decrease by ≈0.2 and ≈1.7, respectively (see Tables II and III).

Let us discuss the DOS plots of Fig. 2. In comparison with the hydrogen free alloy, they show that the most prominent feature is a hydrogen-induced split-off state below the *d* metal band (see the arrows in Fig. 2) which is more visible on the (111) plane. This state is more developed in the Pd projection in all the surfaces [see Fig. 2(c)]. The total DOS for (100) and (110) surface is almost the sum of the individual contributions. The (111) Pd terminated surface present a total and Pd projected DOS similar to the Fe terminated surface [see Fig. 3(a)]. The Fe projection changes with a broadening in the *d* states.

Regarding the bonding, Fig. 4 shows the crystal orbital overlap population (COOP) curves for metal-metal atoms close to H and the metal–H bonds. The interaction between Pd and H is stronger in (100) and (111). The more important Fe-H interaction occurs on the (110) surface. The Fe-Pd intermetallic bond is similar in (100) and (110), while almost no bonding is present in the (111) surface. The Pd-H and Fe-H interaction is always almost bonding. The metal–metal bonds do not change when H is present; only a weakening in Pd–Pd bond is observed in the (111) surface. H is bonded to Pd in the (100) and (111) with similar OP. In the case of the (111) Pd terminated surface there are no Fe–H bonds where the Pd–H bond OP has the higher value of all the considered surfaces. The COOP plots also show that H resides on the Pd surface because it does not alter the Fe-Fe OP. The Fe–H bond is not developed in the (100) plane (see also Table III).

In a previous paper[2] we studied the adsorption of H on the fct alloy surfaces. The most stable plane for the H adsorption is the (100), which is close in energy to the (110).

The H is located at 0.80 Å above the top metal layer. However, in the (110) case, the H is located 0.80 Å below these metal layers. The H adsorption on the plane (111) plane is almost 50% less stable in energy than in the former planes.

The orbital compositions of Fe and Pd atoms show little change after H adsorption. However, in the FePd(110)-H case the Pd 5*s* orbital changes by ≈−0.30. The Fe atoms remain the same except in the (111) case, in which the 4*p* and 3*d* populations decrease by 0.15 and 1.00, respectively.

The total DOS for the planes (100) and (110) are similar, the (111) case being much more dispersed. The total DOS for (110) surface is almost the sum of the individual contributions.

Regarding the bonding, the interaction between Pd and H is stronger than that of Fe and H. There is almost no Fe–H bonding on (100) and (110) surface; however, in the (111) plane, the Fe-H OP (overlap population) is 1/3 of the Pd-H OP. The intermetallic bond is more affected than in the former case.

The present calculations allow us to predict the preferable surface location of H and orbital composition of electronic

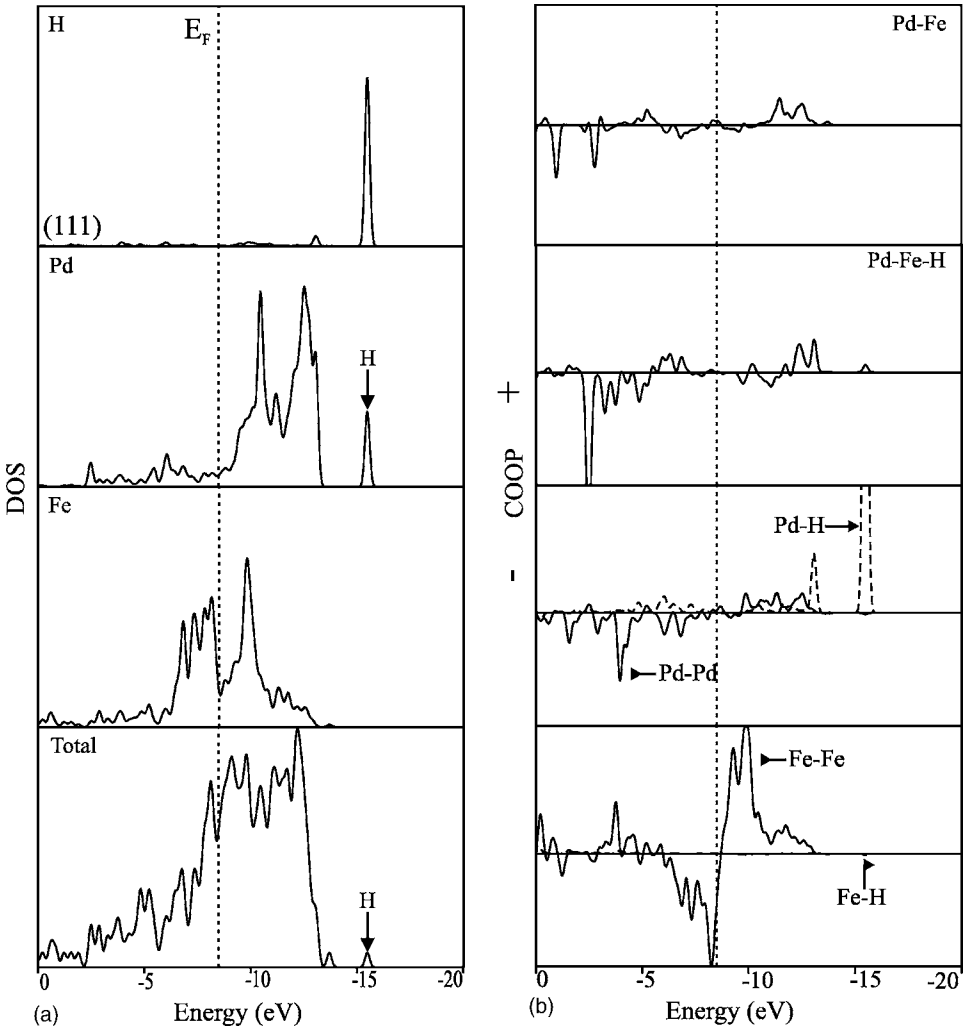

FIG. 3. Total and projected DOS of a Fe-Pd alloy with H adsorbed on the (111) surface (Pd terminated) (a). Metal-metal and metal-H COOP curves for the fcc structure (111) Pd terminated surfaces with and without H (b).

states. The H bonds mainly to Pd atoms and the more influenced metal–metal bond is Pd–Pd on the (100) and (110) surfaces.

Hayashi *et al.* have experimentally determined that Pd-coated Fe films have almost null H permeability.[28] In our previous calculation using a Fe-Pd interface, we have shown that the energy barriers for H diffusion from Pd to Fe are quite high[29] and prevent H migration to the bulk of Fe. Our present calculations have shown that Pd terminated (111) surface only adsorbs H, while the interaction with the Fe layer is almost null. As in pure Pd surfaces our results demonstrate that there are several forms of activated H bound to the catalytic surface.[30]

The atomic charges on hydrogen atoms and Pd–H and Fe–H bonds occupation reflect generally the adsorption geometries, and are very similar for similar coordination complexes on different crystal faces. These data indicate rather local bonding character of hydrogen interaction. The energetic differences for similar coordination positions on different crystal faces arise from the hydrogen-induced changes in the interatomic bonds between nearest palladium atoms.

As in pure Pd or Fe surfaces, the COOP curves show that in the metal-H system the predominant Pd–H or Fe–H bonding character is contained in the split-off bond below the metal band.

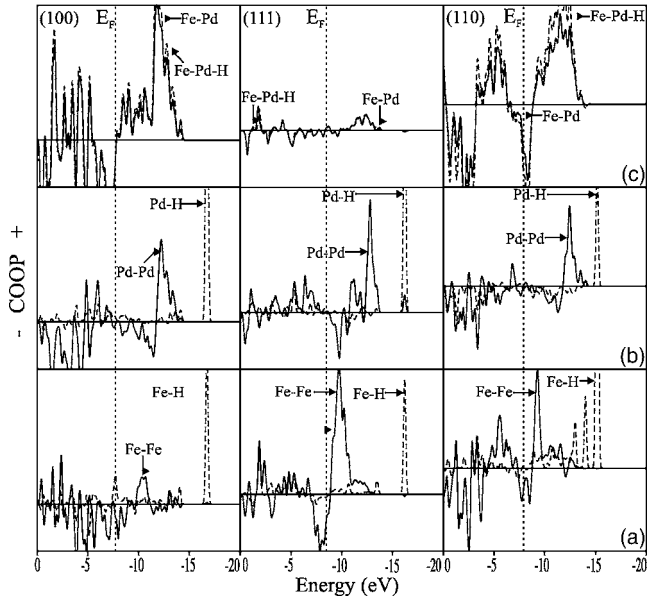

FIG. 4. Metal-metal and metal-H COOP curves for the fcc structures with H adsorbed. Fe-Fe and Fe-H (a); Pd-Pd and Pd-H (b); Fe-Pd and Fe-Pd-H (c). The scale in (111) and (110) planes has been magnified for better viewing.

IV. CONCLUSIONS

The adsorption on four FePd alloys surfaces was considered. H is adsorbed on top of the (110), (111) fcc surfaces and bridged on the (100) surface. In the case of fcc alloy surface, the adsorption alloy is in a bridge position. The Pd-H and the Fe-H distances are in agreement with experiment results in pure metals.

The H develops small split-off states below the *d*-metal bands. The metal–metal OP bonds do not change in the fcc surfaces. In the other stable alloy structure (fct) the intermetallic Fe–Pd bond decreases 27%, while the Pd–Pd bond decreases 70% when H is adsorbed. The geometrical array makes possible the hybridization of Fe and Pd in the fct (111) surface.

We have not considered surface segregations or reconstructions on the surface because, according to experimental data, there is no visible interdiffusion of Fe into the Pd layer.[8] Except for Pd(111) terminated surface, the H is located below the surface plane, which is similar to that reported for TiFe surfaces covered by a Pd monolayer.[10]

Regarding H reactivity in the hydrogenation of unsaturated C–C bonds on TM catalysis, further investigations are under progress. That research will include variable H coverage and temperature effects.

ACKNOWLEDGMENTS

This work was supported by ANPCyT (PICT 12-09857B), UNS-Física and Fundación Antorchas. The authors acknowledge support from CONICET.

APPENDIX:

The calculations were carried out using the atom superposition and electron delocalization tight-binding method (ASED-TB) formalism.[31] This semiempirical method is an improvement of the extended Hückel tight binding (EHTB) method.[32–37]

The adiabatic total energy difference is defined as follows:

$$\Delta E_{\text{total}} = E(\text{FePdH}) - [E(\text{FePd}) + E(\text{H})] + \Sigma E_{\text{repulsion}},$$

where E is the total energy of the system (including electrostatic repulsion).

Although the ASED-TB method is *quite approximate*, the analysis of orbital interactions by this technique seems to be reasonably *reliable*. Our group has used this methodology in previous calculations for the Fe-H system.[38–42] In a recent paper, we have computed, under the ASED approximation, the H trajectories in gamma-Fe.[43] Our results match *qualitatively* those from *ab initio* calculations of Elsässer *et al.* in iron hydrides.[44] The structure and properties of bulk bcc Fe, fcc Pd, and FePd alloys were calculated in order to establish the reliability of the methodology employed, as well as to determine suitable converged values of computational parameters to be used in the subsequent determination of the hydrogen position. The strength of ASED or EH is in fact its transparency, not accuracy, and the main objective of this work is to provide a *qualitative picture* of H interaction on the Fe-Pd fcc surfaces. Our recent DFT calculation for the H-Fe(bcc) (Ref. 45) interactions have shown an excellent agreement with our previous EH calculations.[39] In a recent paper we have computed, under the ASED approximation, the H diffusion trajectories in fcc Fe. Our trajectories show a good agreement in shape and energy barriers with those reported by Elsässer *et al.*[44]

Preliminary DFT calculation of our group predicts the same H localizations in Fe, Pd, and Fe-Pd alloys as the approximate method of the present paper.[46] In a similar manner, cluster calculations with EH method show that the energetics of the most stable adsorption at the zero-coverage limit is very close to that at higher coverage, in agreement with coverage dependencies obtained at the DFT level of theory.[30]

The calculations were implemented with the YAEHMOP program.[47] All *k*-space integrations were performed in the irreducible wedge of the first Brillouin zone (BZ). Within this zone 75 *k* points for fcc alloy and 60 *k* points for the fct alloy were used. The *k*-points set were generated according to the geometrical method of Ramirez and Böhm.[48,49]

*Email address: cajuan@criba.edu.ar

[1] J. H. Sinfelt, *Bimetallic Catalysis: Discoveries, Concepts and Applications* (Wiley, New York, 1983).
[2] E. A. Gonzalez, P. V. Jasen, N. J. Castellani, and A. Juan, Solid State Commun. **131**, 81 (2004).
[3] D. Wang, T. D. Flanagan, and R. Balasubramaniam, J. Alloys Compd. **356**, 3 (2003).
[4] Y. Hayashi, W. M. Shu, T. Shiraishi, and M. Masuda, J. Alloys Compd. **231**, 291 (1995).
[5] W. A. Swansiger and R. Bastasz, J. Nucl. Mater. **85**, 335 (1979).
[6] F. Waelbroeck, K. J. Dietz, P. Wienhold, J. Winter, I. Ali-Khan, H. Merkens, and E. Rota, J. Nucl. Mater. **93**, 839 (1980).
[7] Y. Hayashi, A. Tahara, and M. Ishibashi, in *Hydrogen Effects on Material Behaviour*, edited by N. R. Moody and A. W. Thompson (Minerals, Metals and Material Society, 1990), pp. 11–17.
[8] B. F. P. Roos, A. R. Frank, S. O. Dermokritov, and B. Hillerbrands, J. Magn. Magn. Mater. **198**, 725 (1999).
[9] G. Lee, J. S. Kim, Y. M. Koo, and S. E. Kulkova, Int. J. Hydrogen Energy **27**, 403 (2002).
[10] J. S. Kim, S. O. Oh, G. Lee, Y. M. Koo, S. E. Kulkova, and V. E. Egorushkin, Int. J. Hydrogen Energy **29**, 87 (2004).
[11] S. E. Kulkova, S. V. Eremeev, V. E. Egorushkin, J. S. Kim, and S. O. Oh, Solid State Commun. **126**, 405 (2003).
[12] E. Wicke and H. Brodowsky, in *Hydrogen in Metals*, edited by G. Alefeld and J. Völke (Springer, Berlin, 1973), Vol. II, Chap. 3, p. 73.
[13] P. V. Jasen, E. A. Gonzalez, O. A. Nagel, and A. Juan, Surf. Rev. Lett. **10**, 879 (2003).
[14] P. V. Jasen, E. A. Gonzalez, N. J. Castellani, and A. Juan, J. Mater. Sci. **40**, 2775 (2005).

[15] E. A. Gonzalez, P. V. Jasen, N. J. Castellani, and A. Juan, J. Phys. Chem. Solids **65**, 1799 (2004).
[16] P. Villars and L. D. Calvert, *Pearson's Handbook of Crystallographic Data to Intermetallic Phases*, 2nd ed. (ASM, Metals Park, OH, 1991).
[17] Y. Chen, T. Atago, and T. Mohri, J. Phys.: Condens. Matter **14**, 1903 (2002).
[18] D. Dominguez-Ariza, C. Sousa, N. M. Harrison, M. V. Ganduglia-Pirovano, and F. Illas, Surf. Sci. **522**, 185 (2003).
[19] A. V. Ruban, H. L. Skriver, and J. K. Nørskov, Phys. Rev. B **59**, 15990 (1999).
[20] G. A. Somorjai, *Introduction to Surface Chemistry and Catalysis* (Wiley, New York, 1994), Chap. 3.
[21] A. M. Llois and C. R. Mirasso, Phys. Rev. B **41**, 8112 (1990).
[22] M. Said, M. C. Desjonquères, and D. Spanjaard, Phys. Rev. B **47**, 4722 (1993).
[23] J.-F. Paul and P. Sautet, Phys. Rev. B **53**, 8015 (1996).
[24] D. Tománek, Z. Sun, and S. G. Louie, Phys. Rev. B **43**, 4699 (1991).
[25] M. Skottke, R. J. Behm, G. Ertl, V. Penka, and W. Moritz, J. Chem. Phys. **87**, 6191 (1987).
[26] W. Moritz, R. Imbihl, R. J. Behm, G. Ertland, and T. Matsushima, J. Chem. Phys. **83**, 1959 (1985).
[27] L. Hammer, H. Landskron, W. Nichtl-Pecher, A. Fricke, K. Heinz, and K. Müller, Phys. Rev. B **47**, 15969 (1993).
[28] Y. Hayashi, W. M. Shu, T. Shiraishi, and M. Masuda, J. Alloys Compd. **231**, 291 (1995).
[29] P. V. Jasen, E. A. Gonzalez, O. A. Nagel, and A. Juan, Surf. Rev. Lett. **10**, 879 (2003).
[30] I. Efremenko, J. Mol. Catal. A: Chem. **173**, 19 (2001).
[31] K. Nath and A. B. Anderson, Phys. Rev. B **41**, 5652 (1990).
[32] R. Hoffmann, J. Chem. Phys. **39**, 1397 (1963).
[33] A. B. Anderson and R. Hoffmann, J. Chem. Phys. **60**, 4271 (1974).
[34] W. Lotz, J. Opt. Soc. Am. **60**, 206 (1970).
[35] A. Vela and J. L. Gazques, J. Phys. Chem. **92**, 5688 (1988).
[36] A. B. Anderson, J. Chem. Phys. **62**, 1187 (1975).
[37] A. B. Anderson, Int. J. Quantum Chem. **49**, 581 (1994).
[38] S. Gesari, B. Irigoyen, and A. Juan, J. Phys. D **31**, 2179 (1998).
[39] A. Juan and R. Hoffmann, Surf. Sci. **421**, 1 (1999).
[40] A. Juan, G. Brizuela, B. Irigoyen, and S. Gesari, Surf. Sci. **466**, 97 (2000).
[41] A. Juan, B. Irigoyen, and S. Gesari, Appl. Surf. Sci. **172**, 8 (2001).
[42] S. B. Gesari, M. E. Pronsato, and A. Juan, Appl. Surf. Sci. **187**, 207 (2002).
[43] L. Moro, R. Ferullo, G. Brizuela, and A. Juan, J. Phys. D **33**, 292 (2000).
[44] C. Elsässer, J. Zhu, S. G. Louie, M. Fähnle, and C. T. Chan, J. Phys.: Condens. Matter **10**, 5131 (1998).
[45] M. E. Pronsato, C. Pistonesi, and A. Juan, J. Phys.: Condens. Matter **16**, 1 (2004).
[46] E. Gonzalez, P. Jasen, A. Juan, and N. Castellani (unpublished).
[47] G. A. Landrum and W. V. Glassey, YAEHMOP extended Hückel molecular orbital package is freely available on the WWW at http://sourceforge.net/projects/yaehmop/.
[48] R. Ramirez and M. C. Böhm, Int. J. Quantum Chem. **30**, 391 (1986).
[49] R. Ramirez and M. C. Böhm, Int. J. Quantum Chem. **34**, 571 (1988).